FUDMA Journal of Sciences (FJS)
ISSN online: 2616-1370
ISSN print: 2645 - 2944
Vol. 10 No. 13, July, 2026, pp 325 – 331
DOI: https://doi.org/10.33003/fjs-2026-1013-5740

Characterisation of Tin, Iron and Zircon Ore Samples from Selected Mines in Toro Local Government Area of Bauchi State, Nigeria Using X-Ray Fluorescence Analysis

***Amaechi Christian Sunday, Mathew Nnamdi Agu and Jude Okemsinachi Anaegbu**

Department of Physics, Nigerian Defence Academy, Kaduna, Nigeria

*Corresponding authors' email: Amaechisunday215@gmail.com

ABSTRACT

This study characterised tin, iron, and zircon ore samples from three mining sites (Palama, Zalua, and Gumau) in Toro Local Government Area, Bauchi State, Nigeria, using wavelength-dispersive X-ray Fluorescence (WDXRF) analysis. Nine representative ore samples (three per site) were collected, prepared, and analysed to determine their oxide compositions and impurity profiles. The results revealed that SnO_2 concentrations ranged from 30.259 wt.% (Gumau) to 74.926 wt.% (Palama), corresponding to elemental Sn of 23.817–58.966 wt.%; Fe_2O_3 concentrations ranged from 36.145 wt.% (Gumau) to 38.744 wt.% (Zalua), corresponding to elemental Fe of 25.266–27.082 wt.%; and ZrO_2 concentrations ranged from 38.352 wt.% (Zalua) to 57.010 wt.% (Gumau), corresponding to elemental Zr of 28.380–42.187 wt.%. Major impurity oxides identified included SiO_2 (up to 38.120 wt.%), TiO_2 (up to 42.632 wt.%), and Al_2O_3 (up to 7.838 wt.%), while minor impurities included MnO, MgO, and HfO_2. When compared with London Metal Exchange (LME) and ASTM international export-grade specifications, all samples fell below minimum requirements for direct export: tin ores contained 23.82–58.97 wt.% elemental Sn versus the 99.85% standard; iron ores contained 25.27–27.08 wt.% elemental Fe versus the 62.0% minimum; and zircon ores contained 28.38–42.19 wt.% elemental Zr versus the 62.0–66.0% ZrO_2 minimum. The unusually high TiO_2 content (36.1–42.6 wt.%) in the iron ore samples suggests ilmenite or titaniferous magnetite assemblages rather than conventional iron ores. These findings demonstrate that substantial beneficiation is required for these ores to meet international standards. The study provides critical baseline data for mineral processing and industrial utilisation of these Nigerian ore deposits.

Received: 03 July 2026

Accepted: 09 Aug. 2026

Published: 21 Aug. 2026

Keywords: Characterization, Ore, Impurities, X-Ray Fluorescence, Beneficiation, Bauchi State

INTRODUCTION

Bauchi State, located in northeastern Nigeria, lies within the Precambrian crystalline basement complex that characterises much of the country's geological framework. This basement comprises migmatites, gneisses, schists, and Pan-African granitoids, with younger granite ring complexes intruding in several locations (Obaje, 2009). The tin-zircon sand fields occur in the northeastern part of Barakin Ladi district and the Babale district of Bauchi State, while limestone deposits are found in the southern regions (Mallo, 2000). The economic significance of tin, iron, and zircon minerals in Bauchi State lies in their diverse industrial applications, including electronics manufacturing, steel production, and ceramic/refractory industries (Okoli et al., 2023).

Tin (Sn) is a critical metal used primarily in soldering alloys, tin plating, and electronic components, with global demand driven by the electronics and automotive sectors (International Tin Association, 2020). Iron (Fe) remains the backbone of modern infrastructure, serving as the primary raw material for steel production worldwide. Zircon ($ZrSiO_4$), the primary source of zirconium, finds extensive application in foundry sands, refractories, ceramics, and as a source of zirconium metal for nuclear fuel cladding (Siyanbola et al., 2005).

Several studies have characterised Nigerian ore deposits using XRF and other analytical techniques. Ogunleye et al. (2019) reported elemental compositions of tin ores from the Jos Plateau, identifying significant impurity levels of SiO_2, Al_2O_3, and Fe_2O_3 that affect beneficiation efficiency. Adetunji et al. (2021) characterisedItakpe iron ore, finding Fe contents ranging from 58–65 wt.% depending on the beneficiation stage. Okoli et al. (2023) evaluated Nigerian zircon sands for industrial applications, demonstrating that impurity levels directly impact suitability for high-performance refractories and optical applications. Siyanbola et al. (2005) analysed Nigerian zircon samples using energy-dispersive XRF, establishing baseline compositional data for economic evaluation. Uduma et al. (2023) determined tin content in cassiterite from the Ray-Field mining site, Jos, using EDXRF, reporting average SnO_2 concentrations of 34.6 wt.%.

Despite these contributions, comprehensive characterisation of ores from Toro Local Government Area, Bauchi State, specifically the Palama, Zalua, and Gumau mining sites, remains lacking. This gap is significant because: (a) these sites represent active mining areas with substantial artisanal and small-scale mining activities; (b) local processing decisions are currently made without baseline compositional data; and (c) the potential for beneficiation to improve export-grade quality has not been assessed. Furthermore, data on impurity levels are essential for optimising industrial product fabrication and enhancing export potential, ultimately supporting state economic development (Akinola et al., 2022; Olujobi&Irumekhai, 2024).

This study therefore aimed to: (1) determine the oxide concentrations (SnO_2, Fe_2O_3, ZrO_2) and impurity profiles of ore samples from the three mining sites using XRF analysis; (2) calculate the corresponding elemental concentrations for comparison with international standards; (3) compare the purity levels and impurity distributions between the sites; and (4) evaluate the economic viability of these ores against international export-grade specifications (LME, ASTM). The results provide critical baseline data for mineral beneficiation planning and industrial utilisation strategies.

MATERIALS AND METHODS

Study Area and Sample Collection

This study employed an experimental research design to characterise tin, iron, and zircon ore samples from three selected mines in Toro Local Government Area of Bauchi State, Nigeria (coordinates: approximately 9°15′–10°30′ N, 10°30′–11°00′ E). The area falls within the Precambrian basement complex and is known for active artisanal and small-scale mining activities (Obaje, 2009).

A total of nine ore samples were collected, with three representative samples from each mining site (Palama, Zalua, and Gumau), using systematic random sampling to ensure representation of each deposit. Each sample (approximately 2 kg) was collected from active mining pits at depths of 2–5 meters, representing typical working horizons. Samples were labelled, sealed in polyethene bags, and transported to the National Steel and Iron Research Centre, Malali, Kaduna, Nigeria, for preparation and analysis.

Sample Preparation

Sample preparation followed the standard protocol for powder XRF analysis (Laperche&Lemiere, 2021). Each bulk sample was:

i. Crushed using a jaw crusher to reduce particle size to <2 mm
ii. Pulverised in a tungsten carbide ball mill for 5 minutes to achieve <75 µm particle size
iii. Dried at 105°C for 2 hours to remove moisture
iv. Pressed into 32-mm diameter pellets using a hydraulic press at 20 tons of pressure with boric acid backing

To ensure homogeneity, each pulverised sample was quartered and re-ground three times.

XRF Analysis

Quantitative elemental analysis was performed using a Bruker S8 TIGER wavelength-dispersive X-ray fluorescence (WDXRF) spectrometer at the National Steel and Iron Research Centre, Malali, Kaduna, Nigeria. The instrument was equipped with a 4 kW Rh target X-ray tube operating at 50 kV and 50 mA, with an analysis time of 20 minutes per sample.

Calibration and Quality Assurance/Quality Control (QA/QC):

i. ***Calibration Standards***: Certified reference materials (CRMs) including OREAS 501 (iron ore), OREAS 601 (tin ore), and OREAS 701 (zircon sand) were used to establish calibration curves for each element of interest.
ii. ***Matrix correction:*** The fundamental parameters (FP) method was applied to correct for matrix effects (Lachance &Claisse, 1995; Rousseau, 2001).
iii. ***Replicates:*** Each sample was analysed in triplicate; the mean and standard deviation were reported.
iv. ***Drift monitoring:*** Instrument drift was monitored using a secondary standard (SS-1) every 10 samples.
v. ***Detection limits***: Limits of detection (LOD) ranged from Fe_2O_3 (0.01 wt.%), SnO_2 (0.005 wt.%), ZrO_2 (0.005 wt.%), TiO_2 (0.002 wt.%), Al_2O_3 (0.005 wt.%), SiO_2 (0.01 wt.%), MnO (0.002 wt.%), MgO (0.005 wt.%), HfO_2 (0.003 wt.%).
vi. ***Precision***: Relative standard deviation (RSD) for replicate measurements was <5% for all reported oxides.
vii. ***Accuracy:*** Recovery rates for certified reference materials ranged from 95–105% for all elements of interest, confirming calibration accuracy.

Loss on Ignition (LOI): LOI was determined separately using a muffle furnace at 950°C for 2 hours to account for volatiles, organics, and structurally bound water. LOI values ranged from 2.8–5.4 wt.%.

Data Processing

The XRF spectra were interpreted using Bruker SpectraPlus software to quantify oxide concentrations. All results are reported as weight percentages (wt.%) on a dry, LOI-corrected basis. For comparison with international trade specifications, oxide concentrations were converted to elemental concentrations where required using stoichiometric factors:

$Sn = SnO_2 \times 0.787$ (molecular weight ratio: Sn = 118.71, SnO_2 = 150.71)
$Fe = Fe_2O_3 \times 0.699$ (Fe_2 = 111.69, Fe_2O_3 = 159.69)
$Zr = ZrO_2 \times 0.740$ (Zr = 91.22, ZrO_2 = 123.22)

RESULTS AND DISCUSSION

Results

Quality Assurance and Data Quality

The QA/QC results confirmed the reliability of the XRF measurements. Replicate analysis (n=3 per sample) yielded relative standard deviations (RSD) <5% for all major oxides and <10% for trace elements. Recovery rates for certified reference materials ranged from 95–105% for all elements of interest, confirming calibration accuracy. LOI values ranged from 2.8–5.4 wt.%, accounting for mass deficits in the oxide totals.

Elemental Oxide Concentrations

Table 1 presents the oxide concentrations for all analysed samples. All measurements are expressed in weight per cent (wt.%) on a dry, LOI-corrected basis.

Table 1: Oxide Concentrations of Analysed Ore Samples (wt.%, LOI-Corrected)

Site	Ore Type	SnO_2	Fe_2O_3	MnO	SiO_2	MgO	TiO_2	Al_2O_3	ZrO_2	HfO_2	LOI
Zalua	Zircon	0.764	5.450	0.176	38.120	0.000	6.582	4.057	38.352	1.500	4.1
	Iron	0.000	38.744	2.148	6.797	0.000	42.632	5.751	0.130	0.167	3.2
	Tin	56.003	4.169	0.104	9.072	1.114	6.314	3.357	8.171	0.986	3.8
Palama	Zircon	5.852	1.319	0.000	32.554	0.000	2.383	2.767	49.132	1.913	3.5
	Iron	0.053	37.186	0.000	11.456	1.353	38.615	4.946	0.078	0.074	4.2
	Tin	74.926	1.508	0.000	7.952	0.000	0.257	1.305	4.669	0.473	2.8
Gumau	Zircon	7.133	3.156	0.141	16.707	0.000	5.517	1.183	57.010	2.109	3.7
	Iron	0.000	36.145	1.913	8.344	2.084	40.343	7.838	0.229	0.128	4.5
	Tin	30.259	38.276	0.211	9.993	0.352	6.536	5.909	0.151	0.029	5.4

Summary Statistics and Spatial Trends

Table 2: Summary Statistics of Major Oxide Concentrations (wt.%)

Parameter	Tin Ores (n=3)	Iron Ores (n=3)	Zircon Ores (n=3)
Target Oxide	SnO_2: 30.259–74.926	Fe_2O_3: 36.145–38.744	ZrO_2: 38.352–57.010
Mean SnO_2	53.729 ± 22.414	0.018 ± 0.031	4.583 ± 3.251
Mean Fe_2O_3	14.651 ± 19.643	37.358 ± 1.312	3.308 ± 2.067
Mean ZrO_2	4.330 ± 4.012	0.146 ± 0.077	48.165 ± 9.412
Mean SiO_2	9.006 ± 1.124	8.866 ± 2.385	29.127 ± 10.981
Mean TiO_2	4.369 ± 3.205	40.530 ± 2.273	4.827 ± 2.135
Mean Al_2O_3	3.524 ± 2.304	6.178 ± 1.521	2.669 ± 1.436
Mean LOI	4.00 ± 1.31	3.97 ± 0.67	3.77 ± 0.30

Key Trend Observations

Tin Ores

Purity increases from Gumau (30.259 wt.% SnO_2) <Zalua (56.003 wt.%) < Palama (74.926 wt.%).

Iron Ores

Purity increases from Gumau (36.145 wt.%) < Palama (37.186 wt.%) <Zalua (38.744 wt.%).

Zircon Ores

Purity increases from Zalua (38.352 wt.%) < Palama (49.132 wt.%) <Gumau (57.010 wt.%).

The notable enrichment of TiO_2 in all "iron ore" samples (36.1–42.6 wt.%) suggests these deposits may represent ilmenite or titaniferous magnetite assemblages rather than conventional hematite/magnetite ores (Mohd Hasfarisham et al., 2023; Zhang et al., 2021).

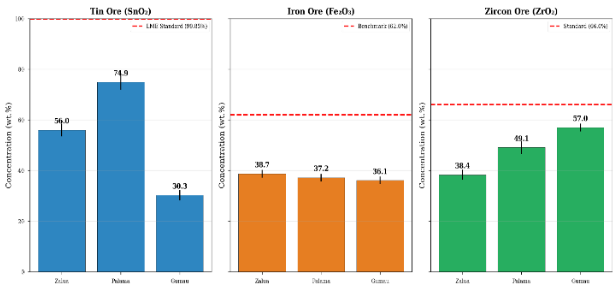

Figure 1: Target Oxide Concentrations by Mining Site

Figure 1 comparison of target oxide concentrations (SnO_2, Fe_2O_3, ZrO_2) in wt.% for tin, iron, and zircon ore samples from Palama, Zalua, and Gumau mining sites, Toro LGA, Bauchi State. Error bars represent standard deviation (n=3). The figure shows significant spatial variability, with Palama exhibiting the highest SnO_2 (74.926 wt.%), Zalua the highest Fe_2O_3 (38.744 wt.%), and Gumau the highest ZrO_2 (57.010 wt.%). Red dashed lines indicate international export-grade standards (LME for Sn, benchmark for Fe, ASTM for ZrO_2). Figure 1 visually confirms the spatial trends observed in the summary statistics. Palama consistently shows the highest SnO_2 concentration, while Zalua and Gumau show the highest Fe_2O_3 and ZrO_2 concentrations, respectively. The wide variation between sites suggests different mineralisation intensities or weathering histories across the Toro LGA.

Calculated Elemental Concentrations

To facilitate comparison with international trade specifications that often reference elemental concentrations, Table 3 presents the calculated elemental concentrations derived from the oxide data using stoichiometric conversion factors.

Table 3: Elemental Concentrations Calculated from Oxide Data (wt.%)

Site	Ore Type	SnO_2 (wt.%)	Calculated Sn (wt.%)	Fe_2O_3 (wt.%)	Calculated Fe (wt.%)	ZrO_2 (wt.%)	Calculated Zr (wt.%)
Zalua	Zircon	0.764	0.601	5.450	3.810	38.352	28.380
	Iron	0.000	0.000	38.744	27.082	0.130	0.096
	Tin	56.003	44.074	4.169	2.914	8.171	6.047
Palama	Zircon	5.852	4.606	1.319	0.922	49.132	36.358
	Iron	0.053	0.042	37.186	25.993	0.078	0.058
	Tin	74.926	58.966	1.508	1.054	4.669	3.455
Gumau	Zircon	7.133	5.614	3.156	2.206	57.010	42.187
	Iron	0.000	0.000	36.145	25.266	0.229	0.169
	Tin	30.259	23.817	38.276	26.755	0.151	0.112
MEAN ± SD							
Tin Ores		53.729 ± 22.414	42.286 ± 17.638	14.651 ± 19.643	10.241 ± 13.731	4.330 ± 4.012	3.205 ± 2.969
Iron Ores		0.018 ± 0.031	0.014 ± 0.024	37.358 ± 1.312	26.114 ± 0.917	0.146 ± 0.077	0.108 ± 0.057

Site	Ore Type	SnO_2 (wt.%)	Calculated Sn (wt.%)	Fe_2O_3 (wt.%)	Calculated Fe (wt.%)	ZrO_2 (wt.%)	Calculated Zr (wt.%)
Zircon Ores		4.583 ± 3.251	3.607 ± 2.558	3.308 ± 2.067	2.313 ± 1.445	48.165 ± 9.412	35.642 ± 6.965

Table 4: Conversion Factors Used for Elemental Calculations

Oxide	Element	Conversion Factor	Calculation
$SnO_2 \rightarrow Sn$	Tin	× 0.787	$Sn = SnO_2 \times (118.71/150.71)$
$Fe_2O_3 \rightarrow Fe$	Iron	× 0.699	$Fe = Fe_2O_3 \times (111.69/159.69)$
$ZrO_2 \rightarrow Zr$	Zirconium	× 0.740	$Zr = ZrO_2 \times (91.22/123.22)$

Trace and Minor Impurities

Other trace impurities identified at concentrations below 1 wt.% included: CrO_3, Co_3O_4, CuO, Nb_2O_3, WO_3, P_2O_5, SO_3, CaO, K_2O, Ta_2O_5, ZnO, Ag_2O, Cl, As_2O_3, CeO_2, and Yb_2O_3. These are reported qualitatively as their concentrations were near or below the instrument's limits of detection for reliable quantitative reporting.

Comparison with International Export-Grade Standards

The comparison of oxide and elemental concentrations with international export-grade standards is illustrated in Figure 2 and summarised in Table 5.

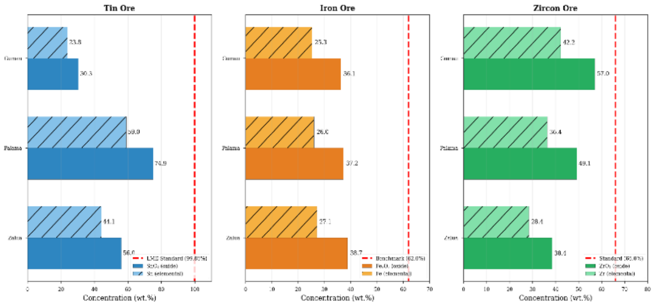

Figure 2: Comparison of Oxide Concentrations (SnO_2, Fe_2O_3, ZrO_2) and Corresponding Calculated Elemental Concentrations (Sn, Fe, Zr) with International Export-Grade Standards (LME and Benchmark Specifications)

The figure demonstrates that all samples fall substantially below the minimum requirements for direct export, with the widest gap observed for tin ores (Palama: 74.926% SnO_2 vs 99.85% standard). Error bars represent standard deviation (n=3).

As shown in Figure 2, the gap between the current ore grades and international standards is substantial for all three commodities. Tin ores show the largest deficit, with even the highest-grade sample (Palama, 58.966 wt.% elemental Sn) falling approximately 41 wt.% below the LME minimum of 99.85 wt.% Sn.

Table 5: Comparison with LME and ASTM Trade Specifications

Commodity	Parameter	Site Range	Export Standard	Status
Tin Ore	SnO_2 content	30.259–74.926%	99.85% minimum (LME)	Below standard
	Elemental Sn	23.817–58.966%	99.85% minimum	Below standard
	Al_2O_3	1.305–5.909%	0.001% max	Exceeds standard
	Fe_2O_3	1.508–38.276%	0.020% max	Exceeds standard
	TiO_2	0.257–6.536%	Not specified	—
Iron Ore	Fe_2O_3 content	36.145–38.744%	62.0% min (Benchmark)	Below standard
	Elemental Fe	25.266–27.082%	62.0% min	Below standard
	SiO_2	6.797–11.456%	5.5% max	Exceeds standard
	Al_2O_3	4.946–7.838%	3.5% max	Exceeds standard
Zircon Ore	$ZrO_2 + HfO_2$	39.852–59.119%	62.0–66.0% min	Below standard
	TiO_2	2.383–6.582%	0.20–0.50% max	Exceeds standard
	Fe_2O_3	1.319–5.450%	0.15–0.25% max	Exceeds standard

Table 6: Summary Comparison of Calculated Elemental Concentrations with Export Standards

Ore Type	Element	Range (wt.%)	Mean ± SD (wt.%)	Export Standard (wt.%)	Status
Tin Ore	Sn	23.817 – 58.966	42.286 ± 17.638	≥ 99.850	Below standard
Iron Ore	Fe	25.266 – 27.082	26.114 ± 0.917	≥ 62.000	Below standard
Zircon Ore	Zr	28.380 – 42.187	35.642 ± 6.965	N/A*	—

Note: *Export Standards for Zircon are Typically Specified as $ZrO_2 + HfO_2$ (≥62–66 wt.%), Not Elemental Zr. The Calculated Zr Values are Provided for Scientific Completeness.

Discussion

Spatial Variability in Ore Quality

The significant variation in target oxide concentrations between the three mining sites (e.g., SnO_2 from 30.259–74.926 wt.%) suggests different mineralisation intensities or weathering histories across the Toro LGA. Palama's elevated tin content (74.926 wt.% SnO_2; 58.966 wt.% elemental Sn) compared to Gumau (30.259 wt.% SnO_2; 23.817 wt.% elemental Sn) may reflect proximity to the primary cassiterite source, greater supergene enrichment, or variations in the host pegmatite composition (Ogunleye et al., 2019; Adedayo et al., 2020). The contrasting trend observed for zircon, where Gumau shows the highest ZrO_2 (57.010 wt.%; 42.187 wt.% elemental Zr), indicates different metallogenic controls for each element, possibly related to sediment provenance or heavy mineral fractionation during weathering and transport (Siyanbola et al., 2005).

However, these interpretations remain speculative without detailed mineralogical (XRD) and petrographic evidence. The small sample size (n=3 per site) limits statistical confidence in these spatial comparisons; future studies should collect more samples across each deposit to confirm these trends.

Implications of the TiO_2 Anomaly

The exceptionally high TiO_2 concentrations observed in the iron ore samples (36.1–42.6 wt.%) are the most striking finding of this study. Typical high-grade hematite ores contain <3 wt.% TiO_2, while commercial ilmenite concentrates contain 44–70 wt.% TiO_2 (Mohd Hasfarisham et al., 2023; Zhang et al., 2021). This suggests that the "iron ore" analysed may actually represent ilmenite ($FeTiO_3$) or titaniferous magnetite (Fe_2TiO_4) deposits.

This distinction has profound implications:

i. Economic Value: Ilmenite is a primary ore of titanium, not iron. The samples may have greater value as a titanium source than as an iron ore. Titanium dioxide (TiO_2) is a high-value product used in pigments, sunscreens, and as a photocatalyst (Gebreslassie&Gebretnsae, 2021).
ii. Processing: Conventional blast furnace ironmaking is not suitable for high-TiO_2 feeds (they cause "elephant skin" formation and furnace stability issues). These ores require different processing routes, such as smelting to produce pig iron and titanium slag (Xi et al., 2021; Talan & Huang, 2022).
iii. Beneficiation: Magnetic separation, gravity concentration, and flotation strategies differ between ilmenite and magnetite/hematite. High-intensity magnetic separation (WHIMS) is typically used for ilmenite upgrading (Sarker et al., 2022).

Recommendation

Mineralogical characterisation by XRD with Rietveld refinement and SEM-EDS is urgently required to confirm the phase assemblages and guide appropriate beneficiation strategies.

Beneficiation Requirements

Table 7: Recommended Beneficiation Routes

Ore Type	Current Grade	Target Grade	Recommended Processing
Tin (Palama)	74.926% SnO_2 (58.966% Sn)	≥99.85% Sn	Gravity concentration + magnetic separation
Tin (Zalua)	56.003% SnO_2 (44.074% Sn)	≥99.85% Sn	Gravity + flotation + magnetic separation
Tin (Gumau)	30.259% SnO_2 (23.817% Sn)	≥99.85% Sn	Flotation + gravity + calcination
Iron (All)	36–39% Fe_2O_3 (25–27% Fe)	≥62% Fe (if Fe ore)	Classification; if ilmenite, WHIMS + flotation
Zircon (Gumau)	57.010% ZrO_2 (42.187% Zr)	≥62% ZrO_2	Spirals + electrostatic separation
Zircon (Palama)	49.132% ZrO_2 (36.358% Zr)	≥62% ZrO_2	Gravity + electrostatic separation

Tin Ores

With SnO_2 levels at 30.259–74.926 wt.% (elemental Sn: 23.817–58.966 wt.%), all samples require beneficiation. For Palama (74.926 wt.% SnO_2), gravity concentration (jigs, shaking tables) followed by magnetic separation to remove iron impurities could potentially upgrade to >90% SnO_2. For Gumau (30.259 wt.% SnO_2), more intensive beneficiation involving froth flotation and calcination would be necessary to meet market specifications (Gebreslassie&Gebretnsae, 2021; Wang et al., 2024).

Iron (Ilmenite) Ores

The high TiO_2 content suggests these are not conventional iron ores. If classified as ilmenite, beneficiation would involve magnetic separation (WHIMS) and flotation to produce ilmenite concentrate (>55% TiO_2) for the titanium pigment or titanium metal industries (Grabarczyk et al., 2023; Duan et al., 2022).

Zircon Ores

With ZrO_2 levels at 38.352–57.010 wt.% (elemental Zr: 28.380–42.187 wt.%), beneficiation involving gravity concentration (spirals, shaking tables) and electrostatic separation could produce marketable zircon concentrates (≥62% ZrO_2) for ceramic and refractory applications (Okoli et al., 2023).

Comparison with Literature

The SnO_2 concentrations reported here (30.259–74.926 wt.%; elemental Sn: 23.817–58.966 wt.%) are comparable to, but generally lower than, values reported by Ogunleye et al. (2019) for Jos Plateau tin ores (62–85 wt.% SnO_2) and Uduma et al. (2023) for Ray-Field cassiterite (average 34.6 wt.% SnO_2). This suggests the Toro deposits may be lower-grade or more weathered.

The Fe_2O_3 values (36.145–38.744 wt.%; elemental Fe: 25.266–27.082 wt.%) are substantially lower than the 60–70 wt.% Fe typical of Itakpe and other Nigerian iron ores (Adetunji et al., 2021), consistent with the ilmenite interpretation.

The ZrO_2 results (38.352–57.010 wt.%; elemental Zr: 28.380–42.187 wt.%) are similar to Nigerian zircon sands reported by Siyanbola et al. (2005) and Okoli et al. (2023), confirming the regional character of these deposits.

Limitations of the Study

Several limitations should be acknowledged:

i. Sample size: Three samples per site (total n=9) is insufficient for robust statistical analysis of spatial heterogeneity. A more comprehensive sampling campaign across each deposit is needed for reliable resource estimation.

ii. Mineralogical data: XRF provides elemental composition but not mineralogy. XRD analysis with Rietveld refinement is essential to confirm phase identities, particularly the TiO_2-bearing phases.

iii. Beneficiation testing: The findings on beneficiation potential are preliminary and require experimental validation through bench-scale beneficiation tests.

iv. Economic analysis: No cost-benefit analysis or net smelter return calculations were performed. Future work should integrate economic modelling.

CONCLUSION

This study successfully characterised tin, iron, and zircon ore samples from Palama, Zalua, and Gumau mining sites in Toro Local Government Area, Bauchi State, Nigeria, using wavelength-dispersive X-ray fluorescence (WDXRF) analysis. The principal findings are:

i. Oxide and Elemental Concentrations:

a. SnO_2 ranged from 30.259 wt.% (Gumau) to 74.926 wt.% (Palama), corresponding to elemental Sn of 23.817–58.966 wt.%

b. Fe_2O_3 ranged from 36.145 wt.% (Gumau) to 38.744 wt.% (Zalua), corresponding to elemental Fe of 25.266–27.082 wt.%

c. ZrO_2 ranged from 38.352 wt.% (Zalua) to 57.010 wt.% (Gumau), corresponding to elemental Zr of 28.380–42.187 wt.%

ii. ***Impurity profiles:*** Major impurities included SiO_2 (up to 38.120 wt.%), TiO_2 (up to 42.632 wt.%), and Al_2O_3 (up to 7.838 wt.%). The elevated TiO_2 in the "iron ores" (36.1–42.6 wt.%) suggests these are actually ilmenite or titaniferous magnetite deposits—a finding requiring mineralogical confirmation.

iii. ***Comparison with standards:*** All samples fell below international export-grade specifications (LME, ASTM), indicating that substantial beneficiation is required:

   a. Tin ores require upgrading from 23.817–58.966 wt.% elemental Sn to ≥99.85% Sn

   b. Iron (ilmenite) ores require beneficiation to produce titanium/iron concentrates

   c. Zircon ores require upgrading from 38.352–57.010 wt.% ZrO_2 to ≥62–66% ZrO_2

iv. ***Spatial variability:*** Significant differences in ore quality between sites suggest varying geological controls; Palama appears most promising for tin (58.966 wt.% Sn), Gumau for zircon (42.187 wt.% Zr; 57.010 wt.% ZrO_2), and Zalua for iron/titanium (27.082 wt.% Fe; 38.744 wt.% Fe_2O_3).

The results provide valuable baseline compositional data for mineral processing planning and industrial utilisation. However, the small sample size and absence of mineralogical characterisation (XRD, SEM-EDS) limit the interpretive scope. Future studies should expand sampling coverage, conduct mineralogical analysis, and perform bench-scale beneficiation tests to confirm economic viability.

ACKNOWLEDGMENTS

The authors thank the National Steel and Iron Research Centre, Malali, Kaduna, Nigeria, for providing analytical facilities and technical support. The assistance of the mining communities in Toro LGA during sample collection is gratefully acknowledged.

CONFLICT OF INTEREST

The authors declare no conflicts of interest.

REFERENCES

Adedayo, O.S., Ibrahim, A., & Musa, H.A. (2020). Geochemical analysis of tin ore deposits using XRF and AAS techniques. *Journal of Applied Geoscience*, 8(2), 45–54.

Adetunji, A.R., Olatunji, M.I., & Bello, T.K. (2021). Chemical characterisation and beneficiation of Itakpe iron ore in Nigeria. *Nigerian Journal of Mining and Geology*, 57(3), 78–88.

Akinola, A.P., Obams, A., & Ifeanyi, A. (2022). Determination of minerals of cassiterite tailings and its recycling potential using empirical method at Plateau State, Nigeria. *International Journal of Advances in Scientific Research and Engineering*, 8(3), 18–42.

Alhassan, A.B., Abdul, D. B., & Abubakar, M.R. (2026) Structural and Morphological Characterization of Graphene Oxide (rGO), and Nitrogen-Doped Graphene Oxide (N-GO) for Electrochemical Water Treatment. FUDMA Journal of Science-Vol.10 No. 13

ASTM International. (2023). Standard specification for tin, iron and zircon ores for metallurgical use. ASTM D4325-23, Philadelphia, USA.

Duan, J., Farrugia, D., Davis, C., & Li, Z. (2022). Effect of impurities on the microstructure and mechanical properties of a low carbon steel. *Ironmaking and Steelmaking*, 49(2), 140–146. https://doi.org/10.1080/03019233.2021.1982209

Gebreslassie, Y.T., &Gebretnsae, H.G. (2021). Green and cost-effective synthesis of tin oxide nanoparticles: A review on the synthesis methodologies, mechanism of formation, and their potential applications. *Nanoscale Research Letters*. https://doi.org/10.1186/s11671-021-03510-7

Grabarczyk, M., Wlazłowska, E., & Fialek, M. (2023). Electrochemical methods for the analysis of trace tin concentrations—Review. *Molecules*, 28(10), 4161. https://doi.org/10.3390/molecules28104161

International Tin Association. (2020). *Tin production and usage standards*. Retrieved from https://www.internationaltin.org/

Lachance, G.R., &Claisse, F. (1995). *Quantitative X-Ray Fluorescence Analysis: Theory and Application*. John Wiley & Sons.

Laperche, V., &Lemiere, B. (2021). Possible pitfalls in the analysis of minerals and loose materials by portable XRF, and how to overcome them. *Minerals*, 11(1), 33. https://doi.org/10.3390/min11010033

London Metal Exchange (LME). (2022). *LME Tin Contract Specification*. Retrieved from https://www.lme.com

Mallo, S.J. (2000). The younger granite ring complexes of Nigeria and their mineralisation. *Journal of Mining and Geology*, 36(2), 145–154.

Mohd Hasfarisham, A., Saidin, M., Abdullah, J., & Jusoh, A. (2023). X-ray fluorescence (XRF) analysis of iron ore at the Sungai Batu archaeological complex, Bujang Valley, Kedah, Malaysia. *Heliyon*, 9(3), e14850. https://doi.org/10.1016/j.heliyon.2023.e14850Add to Jenni

Obaje, N.G. (2009). *Geology and Mineral Resources of Nigeria*. Springer-Verlag Berlin Heidelberg.

Ogunleye, P.O., Ajayi, T.R., & Gbadebo, A.M. (2019). Elemental composition and impurity profile of tin ores from Jos Plateau, Nigeria. *Journal of Mineral Science*, 12(1), 33–41.

Okoli, B.I., Agboola, O.A., Onwualu, A.P., Bello, A., Sholiyi, O.S., Anye, V.C., & Yusuf, O.T. (2023). Characterisation of Nigerian zircon sand and its suitability for different industrial applications. *Minerals*, 13(6), 711. https://doi.org/10.3390/min13060711

Olujobi, O.J., &Irumekhai, O.S. (2024). Strategies and regulatory measures for combating illicit mining operations in Nigeria: A comprehensive legal perspective. *Resources Policy*, 91, 104876. https://doi.org/10.1016/j.resourpol.2024.104876Add to Jenni

Rousseau, R.M. (2001). Fundamental parameter methods in X-ray fluorescence analysis. *Spectrochimica Acta Part B*, 56(6), 861–883. https://doi.org/10.1016/S0584-8547(01)00233-6

Sarker, S.K., Haque, N., Bhuiyan, M., Bruckard, W., & Pramanik, B.K. (2022). Recovery of strategically important critical minerals from mine tailings. *Journal of Environmental Chemical Engineering*, 10(3), 107622. https://doi.org/10.1016/j.jece.2022.107622

Siyanbola, T.O., Adekola, F.A., & Bale, R.B. (2005). Energy-dispersive X-ray fluorescence analysis of samples of Nigerian zircon. *Nuclear Instruments and Methods in Physics Research Section B*, 239(4), 426–432. https://doi.org/10.1016/j.nimb.2005.06.022

Talan, D., & Huang, Q. (2022). A review of environmental aspects of rare earth element extraction processes and solution purification techniques. *Minerals Engineering*, 180, 107510. https://doi.org/10.1016/j.mineng.2022.107510

Uduma, A.U., Jacob, A.G., & Uduma, M.B. (2023). Energy-dispersive X-ray fluorescence analysis (EDXFA) of tin content in cassiterite obtained from Ray-Field mining site, Jos. *FUDMA Journal of Sciences*, 1(1), 185–188.

Wang, Y., Yu, W., Wang, C., Chen, F., Ma, T., & Huang, H. (2024). Defects in photoreduction reactions: Fundamentals, classification, and catalytic energy conversion. *eScience*, 4(3), 100289. https://doi.org/10.1016/j.esci.2024.100289

Xi, F., Li, S., Ma, W., Chen, Z., Wei, K., & Wu, J. (2021). A review of hydrometallurgy techniques for the removal of impurities from metallurgical-grade silicon. *Hydrometallurgy*, 201, 105588. https://doi.org/10.1016/j.hydromet.2021.105588

Zhang, B., Shi, J., Jiang, Y.R., Zhou, J.G., & Li, S.Q. (2021). XRF analysis of impurity metal elements in iron-based alloy. *Open Access Library Journal*, 8, e7846. https://doi.org/10.4236/oalib.1107846